Unraveling the effects of blue light in an artificial solar background light on growth of tomato plants

Pavlos Kalaitzoglou [a], Craig Taylor [a], Kim Calders [b], Maikel Hogervorst [a], Wim van Ieperen [a], Jeremy Harbinson [c], Pieter de Visser [d], Celine C.S. Nicole [e], Leo F.M. Marcelis [a,*]

[a] Horticulture and Product Physiology Group, Wageningen University, Wageningen, The Netherlands
[b] CAVElab - Computational & Applied Vegetation Ecology, Faculty of Bioscience Engineering, Ghent University, Belgium
[c] Laboratory of Biophysics, Wageningen University, Wageningen, The Netherlands
[d] Business Unit Greenhouse Horticulture, Wageningen University & Research, Wageningen, The Netherlands
[e] Signify Research B.V., Eindhoven, The Netherlands

ARTICLE INFO

ABSTRACT

While the use of narrowband irradiance regimes containing different blue light fractions has proven useful to unravel blue light effects on plants at a fundamental level, it does not quantify the responses to blue light under natural daylight conditions. The objective of this study is to understand the blue light growth responses by combining photosynthetic measurements with measurements of whole plant light absorption in a simulated daylight spectrum enriched with different levels of blue light. To achieve this, tomato plants were grown under six different combinations of artificial solar light and blue LED light. Light treatments were defined by the blue light (400–500 nm) fraction of total photosynthetic photon flux density (400–700 nm) and included 27 % (no additional blue LED), 28 %, 31 %, 38 %, 43 % and 61 % blue light with a total photosynthetic photon flux density of 100 µmol m^{-2} s^{-1} in all treatments. Whole plant light absorption was estimated by using ray tracing simulation combined with measured 3-dimensional structure of the plant and optical properties of the leaves. The total dry weight of the plants decreased linearly with the increase of blue light fraction; the dry weight of the plants grown under 27 % blue being 1.6 times greater than that of the plants grown under 61 % blue. This large difference was related to lower light absorption by the plants when fraction blue light increased, due to more compact morphology, i.e. lower leaf area, leaf length/width ratio and shorter stem. Light-limited quantum yield and maximum photosynthetic capacity were not affected by blue light fraction. In the case of the latter, which in other studies has often been found to be positively related to blue light fraction, it may be that the blue light fraction already present in the daylight source had saturated this response. Overall, increasing the blue light fraction in a solar light background decreases growth mainly through its effect on plant morphology and light interception. It remains to be elucidated whether the responses observed using the low growth light intensity in the present study are maintained in high light growth environments more characteristic for tomato growth and production.

1. Introduction

Light is not only the source of energy for photosynthesis but also a source of information about the plant's environment. Since leaves absorb red and blue light strongly but far-red light only weakly, plants themselves greatly modify the natural light environment through the canopy in a wavelength dependant manner by acting as selective optical filters. For example, the particularly weak absorption of far-red light relative to shorter wavelengths means that transmitted light is relatively enriched with far-red light. In contrast, leaves in the upper canopy, which are exposed to direct sunlight, are exposed to a comparatively red and blue-enriched spectrum. These spectral signatures associated with either shade or direct sunlight are translated by various photoreceptors into physiological changes of adaptive benefit. For example, the red:far-red ratio – high in direct sunlight but low in shade – is sensed by phytochrome which triggers etiolation when this ratio is low. The obvious adaptive benefit of this 'shade avoidance syndrome' (SAS) (Smith, 1982) is the potential for improved light capture by at least

maintaining a similar height to neighbouring plants (Nagashima and Hikosaka, 2011). Although less well characterised than the impact of the red:far-red ratio on SAS, blue light depletion also provides similar information about shading and has been associated with the SAS phenotype (Keller et al., 2011; Keuskamp et al., 2012, 2011). For example, Arabidopsis grown using a spectrum containing reduced blue light resulted in comparatively more hypocotyl elongation (Pierik et al., 2009) whereas increasing the fraction of blue light in tomato using a white light or red light mixture had the opposite effect by decreasing plant height (Snowden et al., 2016). Snowden et al. (2016) also observed that petiole length and leaf area index (LAI) decreased under higher blue light fractions. Similarly, several other authors have confirmed the occurrence of reduced stem elongation and increased tomato plant compactness when the fraction of blue light increased, either in narrowband blue:red combinations or under broadband light (Glowacka, 2004; Hernandez et al., 2016; Kaiser et al., 2019; Nanya et al., 2012). These photomorphogenic responses to blue light are known to be regulated by cryptochrome (Ahmad et al., 2002).

At the leaf level, chloroplast movement from the anticlinal position to the periclinal position is mediated by phototropin (Suetsugu and Wada, 2013). Stomatal opening, though not exclusively an effect of blue light, is also mediated by phototropin in the guard cells. An action spectrum for stomatal opening in *Xanthium strumarium* showed that blue light exerted a considerably stronger effect on stomatal opening than red light (Sharkey and Raschke, 1981). Those authors reported that the peak efficacy in the blue region was about 10 times greater than the peak in the red region. At the thylakoid level, blue light has been shown to create 'sun type' chloroplasts compared with red light alone; these are chloroplasts which bear the architectural features of chloroplasts produced under high light i.e. smaller grana stacks and less lamellae (Lichtenthaler et al., 1980). These changes at the thylakoid level are consistent with a higher maximum photosynthetic capacity (Amax). In a blue light dose-response study, Amax in cucumber increased as the blue light fraction increased from 0% to 50 % in a red light background (Hogewoning et al., 2010b). In similar studies Amax in spinach increased when the fraction of blue light was increased up to 33 %, and compared to rice grown under red light adding 25 % blue light increased photosynthetic capacity by 88 % (Matsuda et al., 2004, 2007).

Under low light conditions, however, light-use efficiency of photosynthesis (and overall light capture), rather than Amax, is relevant to growth. In the short-term, blue light is known to drive photosynthesis under light-limited conditions less efficiently than red (Hogewoning et al., 2012; Hoover, 1937; Inada, 1976; McCree, 1971). This is due, at least in part, to the absorption by carotenoids which transfer energy to chlorophyll molecules with less efficiency (ca. 70 %) than chlorophyll to chlorophyll energy transfer (Croce et al., 2001). In the longer term, however, red irradiance alone results in abnormal PSII functioning as evidenced by suppressed Φ_{PSII} which manifests as reduced Φ_{CO2} and dysfunctional stomata compared with blue-red light mixtures (Hogewoning et al., 2012). When red light was supplemented with 25 % blue light the rate of light-limited photosynthesis in rice increased by 53 % (Matsuda et al., 2004).

The wide variety of blue light responses across different scales makes blue light a potentially useful spectral tool with which to explore relationships between photosynthetic and photomorphogenic effects at the whole plant level. While the use of narrowband irradiance regimes containing different blue light fractions has proven useful in unravelling blue light effects at a fundamental level, these studies do not quantify the responses to blue light under natural daylight conditions. Since natural daylight already contains approximately 27 % blue light (Hogewoning et al., 2010a), it is not known whether the addition of more blue light would enhance the potentially already saturated blue light responses even at low daylight levels. This study adopts a holistic approach to understanding blue light responses at the whole-plant level by combining photosynthetic measurements at leaf level with estimations of whole plant light absorption in a simulated daylight spectrum

with, and without, different doses of blue light supplementation. This approach quantitatively relates photomorphogenic responses to whole plant absorption and allows for the disentanglement of the contribution of photosynthetic and photomorphogenic changes to whole plant biomass.

2. Materials and methods

2.1. Plant material and growing conditions

Tomato seeds (*Solanum lycopersicum* cv. Moneymaker) were sown in rockwool blocks (7 cm · 7 cm · 7 cm) (Grodan, Roermond, The Netherlands) and covered with a layer of vermiculite. Sown blocks were placed in a climate chamber under fluorescent tubes (TLD 36 W/840 HF, Philips, The Netherlands). The photosynthetic photon flux density (PPFD) at the rockwool level was 100 µmol m^{-2} s^{-1} and the photoperiod was 16 h. The air temperature and relative humidity in the climate chamber were set to 20 °C, and 70 %. The atmospheric CO_2 concentration was ambient. A week later, when seedlings had emerged, a group of the most homogeneous seedlings were transferred to a different climate chamber and placed in groups of five inside plant growth tents (160 cm · 80 cm · 80 cm). The seedlings remained in the growth tents for 30–32 days after sowing, having developed at least seven leaves longer than 1 cm.

The measured average air temperature in the growth tents was 23.5 °C and the average relative humidity 66.5 %. CO_2 concentration was ambient. Plants were irrigated daily at 8:00 AM for 10 min by ebb and flood technique, using a Hoagland solution (EC 1.2, pH 5.9). Inside each tent, a transparent, spectrum-neutral (400–800 nm) heat screen above the plants separated the climates of the plant compartment (bottom) from the light source compartment (top), blocking part of the radiative heat transfer to the plants (Sonneveld et al., 2006). In both compartments, two 80 mm fans were used to exchange air between the tent and the growth chamber. Additionally, the bottom compartment was equipped with four extra fans (80 mm, 12 V) to ensure a homogenous distribution of air temperature.

2.2. Light treatments

Each growth tent was equipped with a plasma lamp (AS1300, Plasma International GmbH, Offenbach am Main, Germany), suspended 153 cm above the rockwool blocks, providing an artificial solar (AS) broadband spectrum (Fig. 1). Furthermore, there was an array of blue (B) LEDs (a prototype design, Philips, Eindhoven, The Netherlands), suspended 93 cm above the rockwool blocks, providing blue light with a peak wavelength at 450 nm. The output of both light sources was controlled by digital controllers. A spectrum-neutral diffusing screen made from disposable non-woven fabric material was placed 5 cm under the LED array. The screen was used to improve uniformity of both intensity and light spectrum in the tent.

All light treatments had equal PPFD and photoperiod (100 µmol m^{-2} s^{-1} for 16-hs). The spectrum of each treatment was adjusted by replacing part of the broadband plasma lamp light with blue LED light. Therefore, the treatments were defined based on the fraction blue (400–500 nm) they contained in their recorded total PPFD (400–700 nm): 27 % (no blue LED), 28 %, 31 %, 38 %, 43 % and 61 %. The light spectrum was measured in every tent at plant apex height, using a spectroradiometer (USB2000 spectrometer, Ocean Optics, Duiven, The Netherlands) (Fig. 1).

Two groups of plants were used for measurements: those for photosynthesis measurements and those for morphology measurements. For plants designated for morphology measurements, PPFD was measured at five locations at plant apex height using a quantum sensor (LI-190, Li-Cor, NE, USA). To maintain constant PPFD and blue light fraction at the apex of every growing experimental plant, both plasma and blue LED outputs were manually adjusted every two days. Additionally, plants
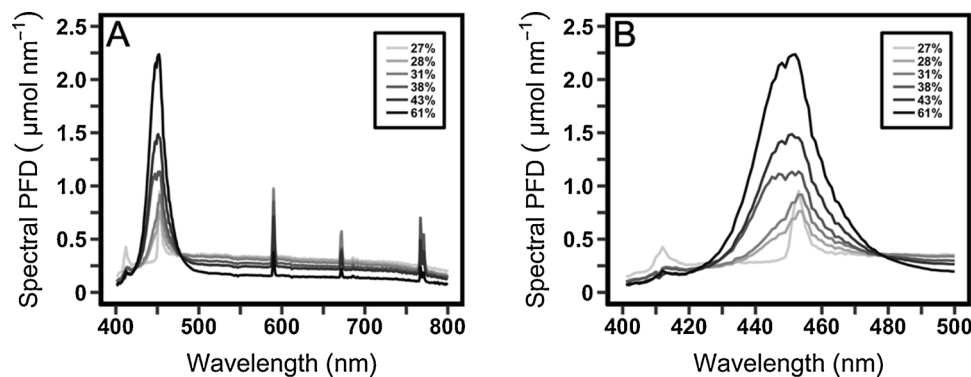
Fig. 1. Spectral light distribution (A: 400 – 800 nm, B: 400 – 500 nm) of plasma lamp without blue light supplementation (containing 27 % blue light) and with blue light supplementation resulting in 28 %, 31 %, 38 %, 43 % and 61 % blue light fraction. [2-column fitting image].

were rotated every two days to minimize the effect of spatial variation in the environment within the tent. Plant positioning in the tents was done in such a way that mutual shading and touching were prevented. The phytochrome photostationary state (P_{fr}/P_{total}) of all light treatments was calculated according to Sager et al. (1988) (0.71, 0.72, 0.72, 0.70, 0.70 and 0.68 for the treatments with 27 %, 28 %, 31 %, 38 %, 43 % and 61 % blue light, respectively). In plants designated for photosynthesis measurements the aim was to maintain a light intensity of 100 µmol m^{-2} s^{-1} at the apex until the third leaf developed, at which point the third leaf became the reference point for light intensity adjustments. Where necessary, the third leaf was gently supported with a wooden dowel to ensure that it was positioned normal to the irradiance.

2.3. Measurements

Thirty days after sowing, plant internode length, petiole length (distance from stem to first leaflet), leaf length (distance from first leaflet to the tip of the last leaflet) and leaf width were measured. The third leaf (counting from the bottom) was selected as representative for analysis since the first and second leaves of tomato plants have distinct and irregular shapes compared to the rest. The internode, hypocotyl and leaf dry weights were measured after oven-drying for 16 h at 70 °C initially, followed by 22 h at 105 °C. The area of every leaf was measured using an area meter (Li-3100, Li-Cor, NE, USA). The specific leaf area (SLA) of every leaf was calculated by dividing its measured area by its measured dry weight (including petiole). For the determination of the leaf number per plant, only leaves with a length of ε1 cm were used.

On the same day, leaf optical properties were measured on other plants. Leaves 1–3 (counting from the bottom) were taken from the plant, immediately placed inside plastic bags and stored for two hours in cold storage room (5 °C). Directly before the measurement, two leaf discs (1 cm diameter; leaf margins and veins were avoided) were taken from the fourth leaflet (counted acropetally) of each stored leaf. Optical properties were measured on both sides of the leaf disc with a custom-built integrating sphere leaf-light absorption system (Taylor et al., 2019). In the range of 400–800 nm the device measured transmittance and reflectance with two integrating spheres, using a light source at a fixed angle and a non-cooled spectrophotometer (USB-4000, Ocean Optics, Dunedin, FL, USA) (Hogewoning et al., 2010a). The acquired data were used to calculate the leaf light absorptance for the light of each treatment. After the measurements, the leaf material was dried like the other plant parts.

An estimation of whole plant light absorption was made based on measurements of plant 3D structure and leaf optical properties, in combination with a ray tracing software mimicking the light environments. A day before the destructive measurements, plant 3D structure was measured. The plants that would be later used for biomass and destructive morphology measurements were first transferred to a 20 m^2 room and subjected to 3D laser scanning. Terrestrial laser scanning

(TLS) is an active remote sensing technique that measures the distance to an object by measuring the time-of-flight of a laser pulse to and from the object (Calders et al., 2015). A RIEGL VZ-400 3D terrestrial scanner (RIEGL Laser Measurement Systems GmbH, Horn, Austria) was used. This time-of-flight scanner has a range up to 350 m, the beam divergence is nominally 0.35 mrad, and the scanner operates in the near infrared (wavelength 1550 nm). This instrument records multiple-returns from each laser pulse to improve the scab resolution (up to four returns per emitted pulse) (Calders et al., 2014). Each plant was scanned from four equidistant locations (minimum separation 1.5 m, 90 degrees azimuth spacing). The TLS data from the individual locations were registered in the RiSCAN PRO software (provided by RIEGL) and points with a deviation of more than 20 were removed to increase the signal-to-noise ratio (Calders et al., 2017) before exporting the final point cloud model for each plant. The plant surface was reconstructed in each point-cloud with MeshLab software (Meshlab, 2014), using the Ball Pivoting Algorithm (Bernardini et al., 1999) (Supplementary Fig. 1). Laplacian smoothing was applied on each reconstructed mesh: for each vertex, the average position with the nearest vertex was calculated in three sequential smoothing steps. Finally, the smoothen meshes were exported as Alias Wavefront Object (*.obj) and Collada File Format (*.dae) file types. The. dae files were imported to SketchUp Make software were the upper angles between petiole and stem were measured.

Light absorption of each plant was computed using a 3D model built in GroIMP modeling platform (Kniemeyer, 2008). This platform allows the use of a multispectral inversed ray tracer, which for this study was set to 20 million rays and a recursion depth (maximum number of light bounces) of 10. The constructed 3D scene mimicked each light treatment, including light intensity and spectrum. Spotlights facing downwards represented the plasma and LED lamps and were situated above the plant according to their positions in the growth tents. The emitted light passed through a transparent cover at ca. 30 cm above the plant model. This model was the smoothed mesh of the 3D scan of each of the treated plants (*.obj file) and was imported in the 3D scene as a wireframe object, with its surface consisting of multiple vertices. For each vertex (or polygon) the measured absorption and reflection were imported as optical parameters. Each 3D model plant was situated inside a box of 1 m · 1 m · 1 m, enclosed by vertical white walls that fully reflected light; black ground floor and ceiling fully absorbed the light. In this approach, all the given light could be traced back in the scene: the light was either absorbed by the plant, reflected to the ceiling or transmitted to the floor (and consequently absorbed by the ceiling and the floor).

2.4. Gas exchange

Gas exchange was measured by custom-made equipment with a leaf chamber similar to that described in Taylor et al. (2019). Actinic light comprised two light sources; artificial daylight was produced by a

plasma lamp identical to the one used for growth, and blue light was produced by LEDs with a practically identical emission spectrum to those used for growth light. The blue LEDs were arranged in an array on a metal-cored printed circuit board. All light sources were coupled to the chamber with glass fibres. Light intensity from the plasma lamp was controlled with built-in electronic control but, since the lamp cannot sustain an arc below a minimum current it was used in combination with a neutral density filter comprised one or more layers of fine wire gauze on an adjustable rotatable disk between the lamp and the optical fibre.

Measurements were taken on third, fully expanded leaves, usually at about 30–32 days after seeds were sown. Two sets of gas exchange measurements were taken on each leaf. The first set of measurements was taken at low O_2 mole fraction (20 mmol mol^{-1}) to inhibit photorespiration while the subsequent second set of measurements on the same leaf were taken at ambient O_2 (210 mmol mol^{-1}). In both cases, the concentration of CO_2 was 400 µmol mol^{-1}, and the concentration of H_2O was set to 18 mmol mol^{-1} (70 % RH) by adjusting the proportion of the incoming airstream which was passed through a bubbler with temperature-controlled water. The remaining gas fraction consisted of N_2. A Li-7000 infrared CO_2/H_2O analyzer (LI-COR, Lincoln, Nebraska, USA), set in differential mode, analyzed incoming and outgoing gas streams. Leaf temperature was monitored using a calibrated infrared (non-contact) thermocouple (Micro IRt/c, Exergen, Watertown, MA, USA) and maintained at 23 °C by circulating water of the appropriate temperature through cavities in the upper and lower chamber halves. Assimilation was measured at five light-limiting irradiances (10, 25, 50, 75 and 100 µmol m^{-2} s^{-1}) at a low O_2 mole fraction. To ensure that these irradiances were light-limiting, light response curves were examined for inflection points at which the response became curvilinear. It was found that these intensities were indeed light-limiting as evidenced by the strong linearity of the assimilation response up to, and including, 100 µmol m^{-2} s^{-1}. The lowest light intensity of 10 µmol m^{-2} s^{-1} was chosen to avoid potential non-linearity associated with the Kok effect at very low light intensities (Kok, 1948). Measurements at ambient O_2 mole fraction were taken using the same light-limiting irradiances but also included higher irradiances of 200, 400, 800, 1200, 1600, and 1800 µmol m^{-2} s^{-1}. Leaves were subjected to each light intensity step for as long as necessary for the rate of gas exchange to reach a steady state. Assimilation (A) and stomatal conductance (g_s) were calculated according to the model of Farquhar et al. (1980). The purpose of low O_2 measurements was to remove the effect of potential differences in photorespiration amongst treatments arising from potential blue-light mediated changes in mesophyll and stomatal conductances.

Maximum quantum yield of CO_2 fixation at low and ambient CO_2 (Φ_{CO_2}) was taken as the slope of a linear regression of the gas exchange-irradiance response curve for the first five light-limiting irradiances (10−100 µmol m^{-2} s^{-1}). Maximum photosynthetic capacity (Amax) for the full light response curves at ambient CO_2 was determined using the non-linear hyperbolic function of Thornley (1976).

2.5. Chlorophyll fluorescence

Chlorophyll fluorescence parameters were measured using a lab-built system comprising a modulated measuring beam and lock-in amplifier. Upon commencement of gas exchange measurement, Fv/Fm was measured in dark adapted leaves. Fm was determined using a saturating flash of 12 000 µmol m^{-2} s^{-1} for 1 s generated by three high-power red LEDs (623 nm, Phlatlight PT120, Luminus Devices, CA, USA) coupled to the chamber by three glass fibres. The intensity of the measuring beam, produced by a red LED (660 nm), was approximately 0.5 µmol m^{-2} s^{-1}. Three GaAsP photodiodes (G1736, Hamamatsu, Hamamatsu City, Japan) with their optical windows covered with RG-9 filters (Schott, Mainz, Germany) were used to detect fluorescence signal. $\Phi_{PSII(LL)}$ was determined at each light step up to and including the highest light-limiting intensity used of 100 µmol m^{-2} s^{-1}.

2.6. Measurement of 820 nm absorption changes and $\Phi_{PSI(LL)}$ estimation

The modulated measuring beam for Δ820 nm was produced using a LED (ELJ-810-228B, Roithner Lasertechnik, Vienna, Austria) modulated at 455 kHz coupled to the chamber by a glass fibre and the signal was detected below the leaf by three silicon photodiodes (BPW 34 FA, Osram, Regensburg, Germany) connected to a selective amplifier containing a 455 kHz ceramic filter (Murata, Kyoto, Japan). Three steady state signal levels were used to estimate $\Phi_{PSI(LL)}$: 1.) The 820 nm signal in the light, 2.) the subsequent and rapid change in 820 nm signal (ΔA820) when actinic light was turned off (i.e. in darkness), and 3.) the signal obtained when a ca. 10 s far-red pulse was applied during darkness to fully oxidise P700. The use of a saturating pulse (5 ms duration using the same saturating pulse as for the chlorophyll fluorescence) was used to oxidise any P700 which may have not been oxidized during the application of far-red light (Kingston-Smith et al., 1999). These absorbance changes were used to estimate $\Phi_{PSI(LL)}$ according to the calculation of Baker et al. (2007).

2.7. Experimental design and statistical analysis

There were six light treatments each with three replicate plots (n = 3), with two replicate plants per plot for measurement of growth, biomass and 3D structure, two for photosynthesis and one for optical properties measurements. Hence, there were in total always six or nine replicate plants per treatment. The plots were distributed over four tents in five separate time periods. Linear regression was applied to the response of plant morphological parameters (plant height, total leaf area etc.) to the fraction of blue light ($P = 0.05$). Additionally, linear regression was applied to the test the correlation between total plant light absorption and plant morphological parameters (plant height and total leaf area, and leaf length, width, length/width and angle) and photosynthesis ($P = 0.05$). For every measured response, the normality of the data was confirmed with Shapiro - Wilk normality test. All analyses were conducted in R (R Development Core Team, 2010). All figures were also created in R using the ggplot2 data visualization package (Wickham, 2016).

3. Results

3.1. Plant growth, morphology and development

Plant height decreased linearly with the increase of fraction blue light ($P < 0.001$) (Figs. 2A,3). The plant height decreased by 55 % and the hypocotyl length by 35 % at the highest (61 %) compared to lowest (27 %) fraction blue treatment. Length, width, and length/width ratio of the third leaf decreased linearly with the increase of fraction blue ($P < 0.05$) (Fig. 2C-E), but petiole length was not affected ($P = 0.053$). The total plant leaf area also decreased linearly ($P < 0.05$), being 30 % lower in plants growing under 61 % compared to plants growing at 27 % fraction blue treatment (Fig. 2F).

The dry weight of plants decreased linearly with the increase of fraction blue light ($P < 0.05$) (Fig. 2B). Plant dry weight decreased by 37 % under the highest compared to lowest fraction blue treatment. Leaf number, specific leaf area and angle of the third leaf (upper angle between petiole and stem) were not affected by the increase of fraction blue ($P > 0.05$) (Table 1). The fraction of dry weight partitioned to the leaves increased linearly with the increase of fraction blue ($P < 0.001$), at the expense of stem (Table 2).

3.2. Leaf light absorptance

The light absorptance per unit leaf area of both the adaxial and abaxial sides of the third leaf increased linearly with the increase of fraction blue light ($P < 0.05$), but relative effects were rather small (Fig. 4). Plants grown under 61 % blue light fraction had a light
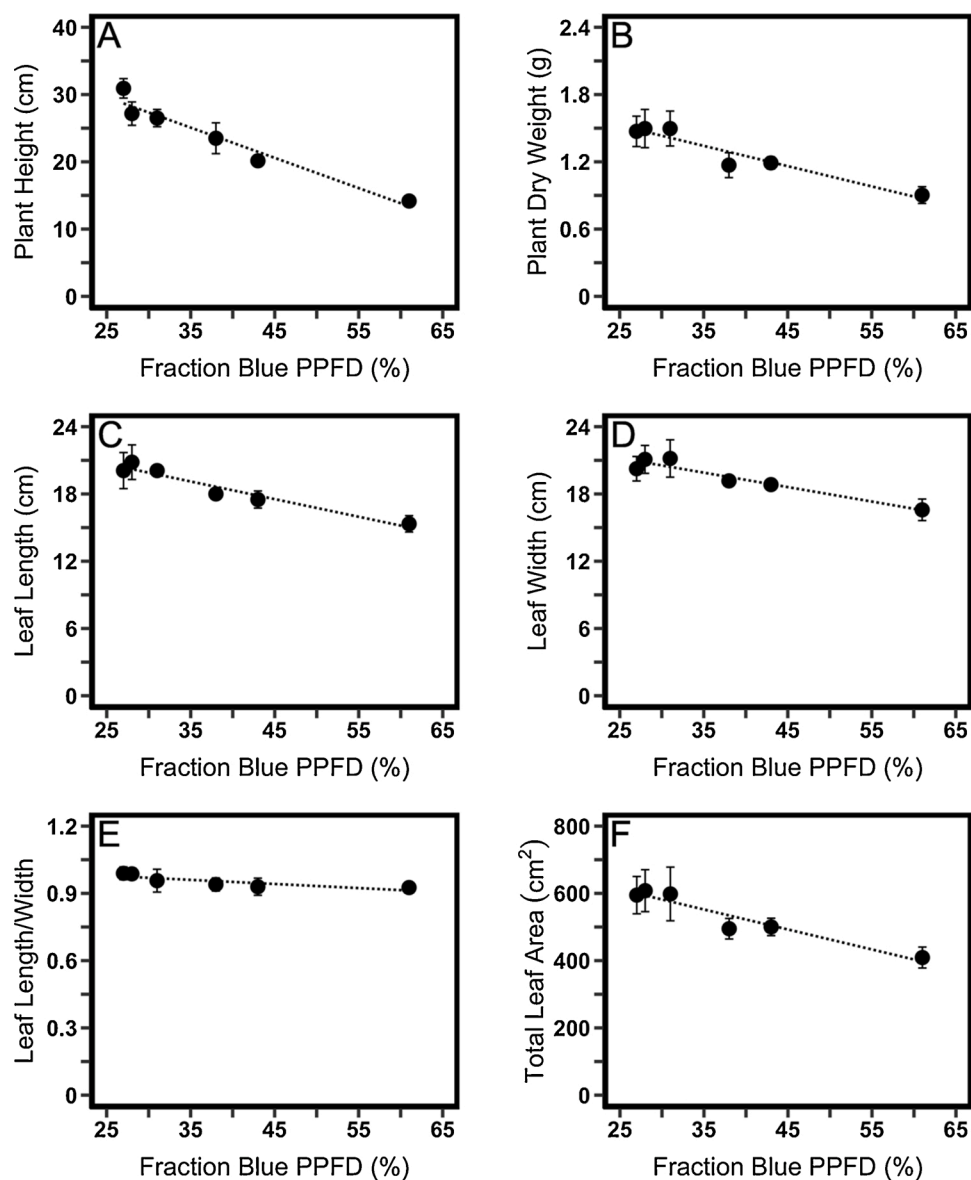
Fig. 2. Effects of fraction blue light on (A) height, (B) dry weight, (C) length of the third leaf counting from the bottom, (D) width of the third leaf counting from the bottom, (E) length to width ratio of the third leaf counting from the bottom and, (F) total leaf area of tomato plants grown for 23 days under a total of $100 \, \mu\mathrm{mol \, m^{-2} \, s^{-1}}$ blue + artificial solar PPFD. Error bars indicate means ± SEM from three plots (n = 3) with two replicate plants per plot. The lines represent significant linear regression (P < 0.05). [2-column fitting image].

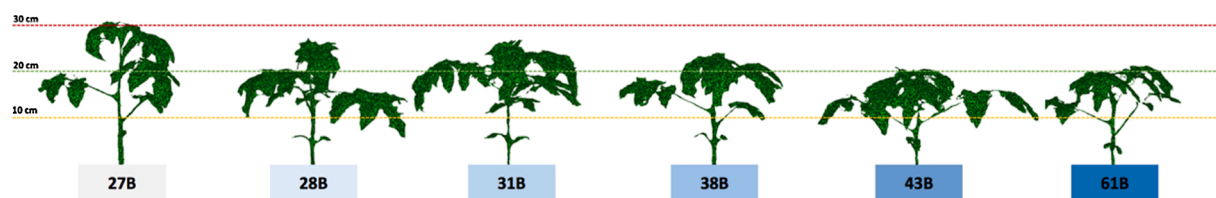**Fig. 3.** Effects of fraction blue light on the architecture of tomato plants grown for 23 days under a total of $100 \, \mu\mathrm{mol \, m^{-2} \, s^{-1}}$ blue + artificial solar PPFD. Images are 3D scans acquired with a terrestrial laser scanner (TLS). The colour of the block under each plant resembles the fraction blue. All 3D scans are presented in Supplementary Fig. 2. [2-column fitting image].

Table 1
Effects of fraction blue light on the leaf number of plants, specific leaf area (SLA) and upper angle between petiole and stem of leaf number 3. The tomato plants were grown for 23 days under a total of $100 \, \mu\mathrm{mol \, m^{-2} \, s^{-1}}$ blue + artificial solar PPFD. Data are means ± SEM from three plots (n = 3) with two replicate plants per plot. P-value indicates the significance of the F-ratio of the linear regression.

	27 %	28 %	31 %	38 %	43 %	61 %	P
Leaf number	6.33±0.17	6.50±0.29	6.50±0.50	6.00±0.00	6.17±0.17	6.00±0.00	0.113
SLA (cm² g⁻¹)	574±4.4	562±26.3	544±21.1	564±18.7	555±12.0	551±27.3	0.576
Leaf angle (°)	67.6±7.6	71.7±4.4	53.4±1.0	62.3±5.6	59.9±7.8	58.3±5.3	0.273

Table 2
Effects of blue light fraction on dry weight partitioning (%) to leaves and stems of tomato plants grown for 23 days under a total of 100 µmol m^{-2} s^{-1} B + AS PPFD. Data are means ± SEM from three plots (n = 3) with two replicate plants per plot. P-value indicates the significance of the F-ratio of the linear regression.

	27 %	28 %	31 %	38 %	43 %	61 %	P
Leaves (%)	71.1±1.01	73.4±0.40	74.3±1.86	75.9±1.24	76.0±1.24	83.1±0.33	<0.001
Stem (%)	28.9±0.69	26.6±0.56	25.7±1.23	24.1±0.83	24.0±1.03	16.9±0.74	<0.001
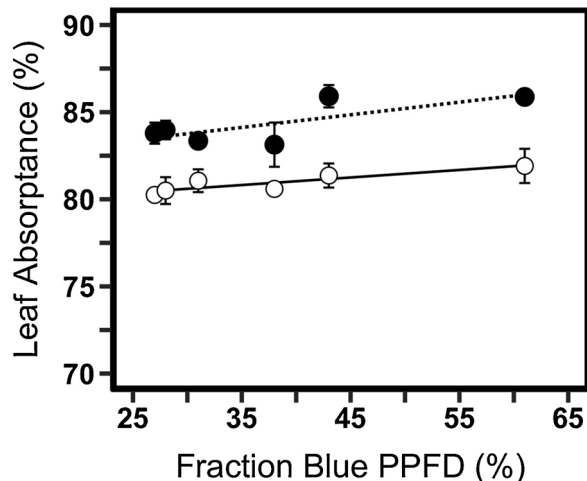
Fig. 4. Effects of fraction blue light on the integrated light absorptance (400 – 700 nm) of the third appeared leaf of tomato plants grown for 23 days under a total of 100 µmol m^{-2} s^{-1} blue + artificial solar PPFD (adaxial side: ●; abaxial side: ○). Error bars indicate means ± SEM from three plots (n = 3) with two replicate plants per plot. The lines (adaxial side: dotted; abaxial side: solid) represent significant linear regression (P < 0.05). [1-column fitting image].

absorptance which was 2.5 % (adaxial) and 2% (abaxial) higher than when grown under 27 % blue light fraction. The spectral distribution of the absorptance did not vary among treatments, hence optical properties of the leaves were not affected by the treatments (data not shown).

3.3. Photosynthesis

Mean Fv/Fm amongst all treatments was 0.78 (SE = 0.004). The response of assimilation to light intensity between 10–100 µmol m^{-2} s^{-1} was highly linear with a mean R^2 of 0.997 (SE = 0.0008), indicating that photosynthesis was light-limited within this range. The light-limited quantum yield of CO_2 fixation ($\Phi_{CO2(LL)}$; µmol m^{-2} s CO_2.µmol photons^{-1}) was substantially higher at 2% O_2 than at 21 % due to the suppression of photorespiration at the lower O_2 concentration (Fig. 5A). The response of $\Phi_{CO2(LL)}$ at the higher O_2 concentration generally mirrored the response at low O_2. $\Phi_{CO2(LL)}$ amongst treatments ranged from 0.064 to 0.069 at 2% O_2 and 0.046 to 0.050 at 21 % O_2. However, the treatment effects on $\Phi_{CO2(LL)}$ were small and not significant. Likewise, $\Phi_{PSII(LL)}$ was similar amongst treatments, ranging from 0.75 – 0.76 at the highest light-limiting intensity used of 100 µmol m^{-2} s^{-1} (Fig. 5B). $\Phi_{PSI(LL)}$, on the other hand, was comparatively more affected by blue light fraction at the same light intensity (Fig. 5C). $\Phi_{PSI(LL)}$ ranged from 0.81 to 0.9 at 2% O_2 and from 0.82 to 0.88 at 21 % O_2 with the lowest efficiency at 31 % and greatest at 61 % blue. $\Phi_{PSI(LL)}$ and $\Phi_{PSII(LL)}$ generally showed opposite trends i.e. when PSII was greatest at 31 % blue, $\Phi_{PSI(LL)}$ was lowest. The excitation balance of PSII and PSI (Fig. 5D), calculated as the yield of PSII divided by the sum of the yield of PSI and PSII, also showed a peak at 31 %. Stomatal conductance (g_s) was highest at 31 % blue (Fig. 5E) while no effect of the fraction blue light in the growth irradiance was observed for the maximum photosynthetic capacity (Amax) (Fig. 5F).

3.4. Plant light absorption

The total plant light absorption decreased linearly (P < 0.01) with the increase of fraction blue light (Fig. 6A). At 61 % blue fraction treatment plants had total light absorption which was 22 % lower than that of plants at 27 % blue fraction. Plant dry weight correlated linearly with plant light absorption (P < 0.01) (Fig. 6B), which correlated linearly with leaf area (P < 0.01) (Fig. 6C). Additionally, the total plant light absorption decreased linearly with a decrease of plant height (P < 0.001) and length, width (P < 0.01) and length/width ratio of the third leaf (P < 0.05) (Supplementary Fig. 3). Total plant light absorption did not correlate with leaf angle or petiole length (P > 0.05). Lastly, plant dry weight correlated linearly with $\Phi_{PSI(LL)}$ (negatively) and photosystem excitation balance (P < 0.05), but not with $\Phi_{PSII(LL)}$, Φ_{CO2} (P > 0.05) (Supplementary Fig. 4).

4. Discussion

4.1. Plant morphology and photosynthesis

Total plant light absorption decreased linearly with the increase of the blue light fraction (Fig. 6A), in agreement with the findings of Snowden et al. (2016). Specifically, total plant light absorption decreased linearly with the decrease of plant leaf area (Fig. 6C), height, third leaf length and width, and length/with ratio (P < 0.05). The results are in accordance with the findings of Sarlikioti et al. (2011) who showed through simulations performed with an FSPM, that increased internode length and leaf length:width ratio increased total light absorption in tomatoes, due to the reduction in leaf mutual shading. In our study, it is safe to conclude that increased blue light fraction induced a set of phenotypic traits that decreased the total light absorption mainly due to decreased leaf area. Although the leaf area decreased linearly with the increase of fraction blue light (Fig. 2F), the percentage of assimilates partitioned to the leaves increased (Table 2). These two responses combined resulted in a decreased SLA (although not significant) as blue light fraction increased (Table 1). Similar responses to increasing fraction blue light under low irradiance (100 µmol m^{-2} s^{-1}) have often been associated with leaf responses to high irradiances (Hogewoning et al., 2010b; Poorter et al., 2009). Moreover, the decrease of leaf area and SLA (or 1/LMA) with the increase of fraction blue light has often been reported (Hernandez et al., 2016; Hernández and Kubota, 2016; Hogewoning et al., 2010a).

Despite the greatly differing spectra used for growth and measurement, the fraction of blue light used for growth and measurement had a negligible effect on $\Phi_{CO2(LL)}$ (Fig. 5A). In cucumber grown under different blue light doses in a red background, $\Phi_{CO2(LL)}$ remained within a narrow range between 0.045 and 0.053, with the lowest values at 0% and 100 % blue (Hogewoning et al., 2010b). The similar $\Phi_{CO2(LL)}$ values obtained in the present study are not surprising given that, individually, the blue light and simulated daylight spectra used drive photosynthesis with similar efficiencies; in the present study ΦCO_2 in simulated daylight of 0.065 (2% O_2) is comparable to that of 0.058 – 0.063 obtained by Hogewoning et al. (2012) when cucumber leaves produced under diverse growth spectra were presented with monochromatic blue irradiance with a peak wavelength of 444 nm. There are however two different reasons for the relative inefficiency of daylight and blue light compared with, for example, red light: in the case of blue light energy transfer from carotenoids to chlorophyll is less efficient than
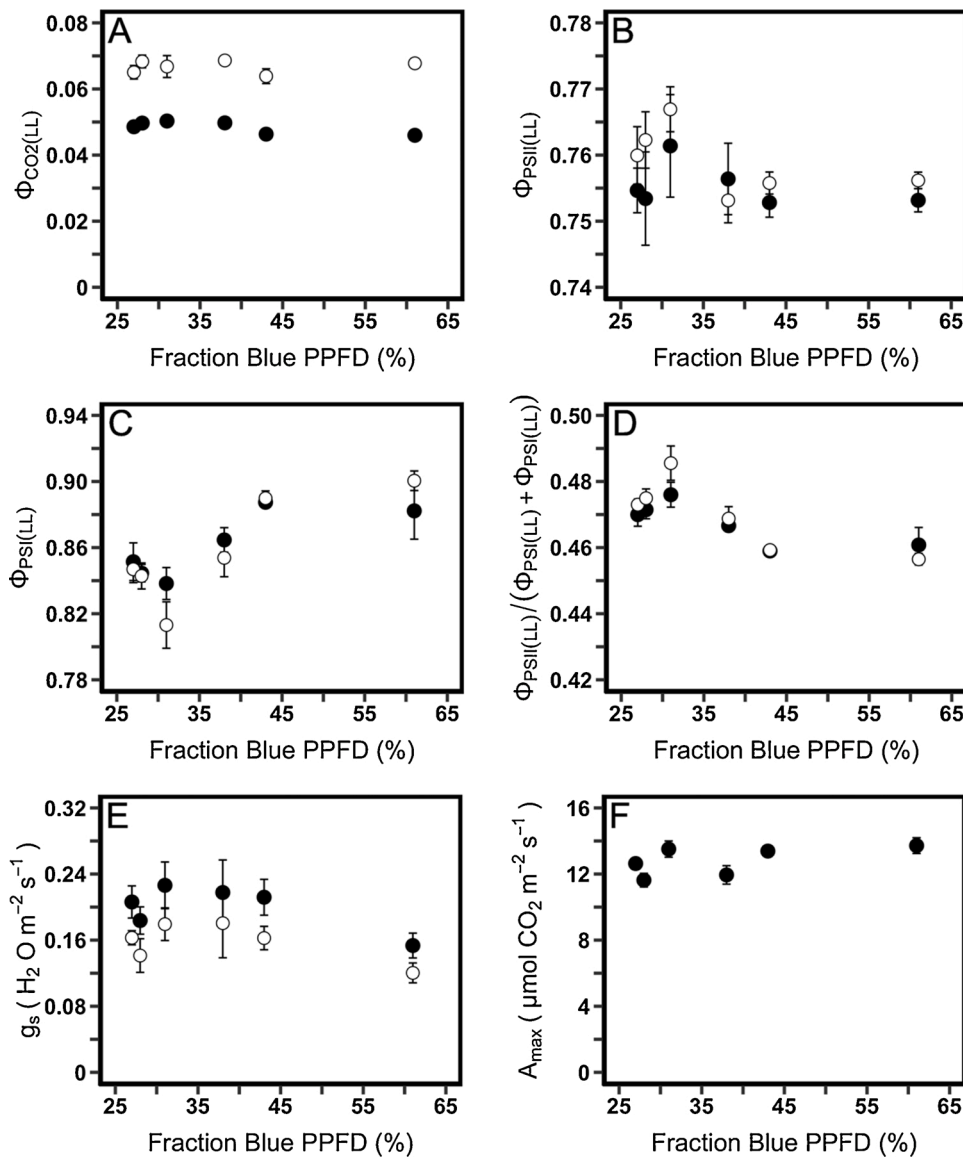
Fig. 5. Effects of different fractions of blue light in actinic irradiance on (A) $\Phi_{CO2(LL)}$; μmol m^{-2} s CO_2.μmol photons^{-1}, (B) $\Phi_{PSII(LL)}$, (C) $\Phi_{PSII(LL)}$, (D) photosystem excitation balance calculated as the fraction of $\Phi_{PSII(LL)}$ relative to the sum of $\Phi_{PSI(LL)}$ and $\Phi_{PSII(LL)}$, (E) stomatal conductance and (F) maximum photosynthetic capacity as determined on tomato leaves grown under the same growth irradiance and spectrum of 100 μmol m^{-2} s^{-1} blue + artificial solar PPFD. Different symbols indicate measurements under 2% ($\circ$) and 21 % ($\bullet$) oxygen levels. Error bars indicate means $\pm$ SEM (n = 3). [2-column fitting image].

chlorophyll-chlorophyll energy transfer (Croce et al., 2001) whereas, apart from blue light, daylight contains other less efficient wavelengths such as green and far-red which, on their own, are used less efficiently for photosynthesis. The relatively small difference in $\Phi_{CO2(LL)}$ between treatments may also be partly due to acclimatory mechanisms which act to improve photosynthetic light-use efficiency and so maximise $\Phi_{CO2(LL)}$ and partly mitigate losses in $\Phi_{CO2(LL)}$. For example, leaves can adjust the relative amounts of PSI and PSII to maintain a high light-use for electron transport and thus a high $\Phi_{CO2(LL)}$ (Chow et al., 1990). The same adjustments could have reduced any potential differences in $\Phi_{CO2(L)}$ arising from the amount of blue light in the growth spectrum, causing leaves to converge upon similar $\Phi_{CO2(LL)}$ values. Amax, on the other hand, has been shown to be a plastic trait which responds strongly to blue light fraction. In the same study by Hogewoning et al. (2010b), Amax was shown to increase up to the 50 % blue light dose treatment and in a similar study Amax in spinach leaves was shown to increase up to 33 % blue light in a red light background (Matsuda et al., 2007). However, a key difference between our study and that of others where narrowband red-blue mixtures were used is that the background artificial daylight spectrum we used comprised 27 % blue light (ie the irradiance between 400 and 500 nm). This is only slightly less than the blue light fraction which resulted in saturation Amax in the study by Matsuda

et al. (2007). It is possible, therefore, that the blue content of our 'white light' background had saturated the blue light mechanisms which contribute to higher Amax. This explanation may also account for the lack of effect of blue light on stomatal conductance, which is otherwise known to be stimulated by blue light (Sharkey and Raschke, 1981). While $\Phi_{PSII(LL)}$ was remarkably similar across the spectra used, $\Phi_{PSI(LL)}$ showed a more varied response (Fig. 5C). The latter can be accounted for by the far-red fraction (700–720 nm) of the white light used which was 5.7 % of irradiance in the spectral range 400–720 nm. Compared to other wavelengths (including blue light) far-red light is known to over-excite PSI compared to PSII (Hogewoning et al., 2012; Laisk et al., 2014). In cucumber leaves, ΦPSI at 720 nm (ca. 0.1 – 0.15) was considerably less than for most wavelengths in the PAR region including 450 nm where ΦPSI was high (>0.9) (Hogewoning et al., 2012). Laisk et al. (2014) calculated PSI absorption to be approximately 0.8 and greater at wavelengths <700 nm whereas at 450 nm this figure was ca. 0.3. Therefore, as blue light fraction increased from 27 % to 61 %, far-red irradiance between 700 and 720 nm decreased from 5.7 % to 2.7 % so decreasing the relative over-excitation of PSI and resulting in an increase in $\Phi_{PSI(LL)}$. This highlights the need to consider not only direct blue light impacts but also indirect effects which inevitably occur in spectral dose response studies in which one irradiance flux is partially
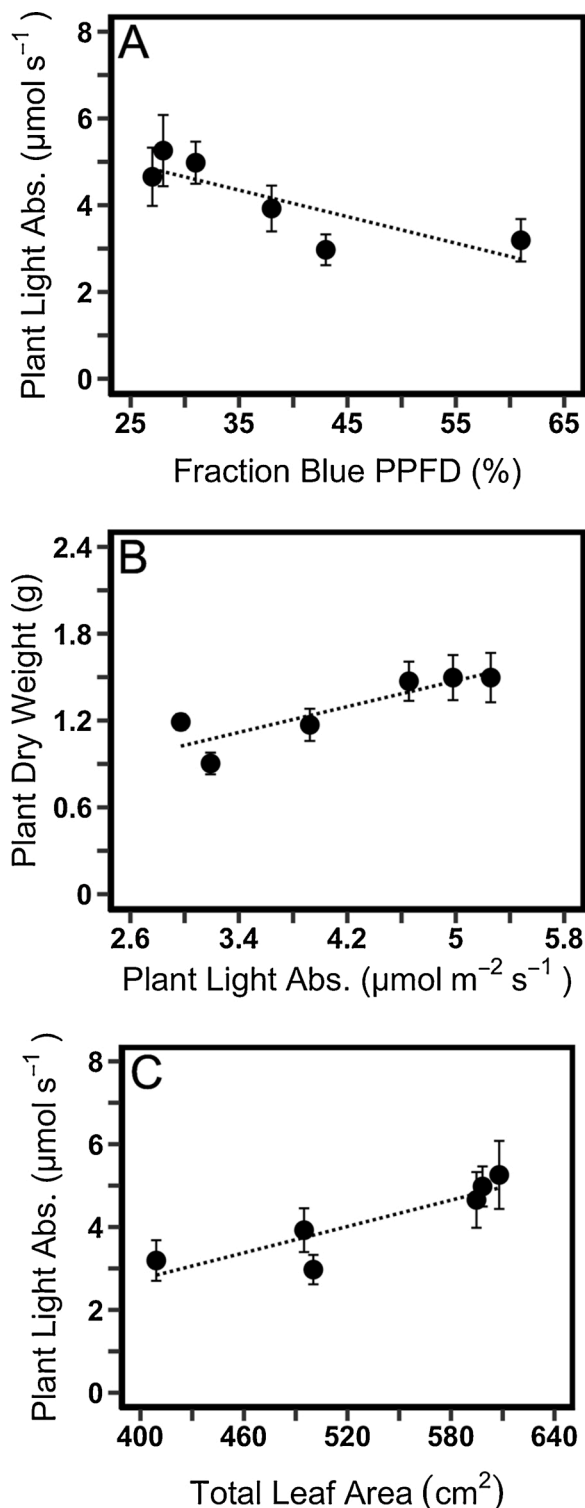
Fig. 6. (A) Effects of fraction blue light on the estimated plant light absorption, (B) effects of the estimated plant light absorption on the plant dry weight and, (C) effects of plant leaf area on the estimated plant light absorption of tomato plants at day 23, when grown under a total of 100 μmol m^{-2} s^{-1} blue + artificial solar PFD. Error bars indicate means $\pm$ SEM from three plots (n = 3) with two replicate plants per plot. The dotted lines represent significant linear regression (P < 0.05). [1-column fitting image].

replaced by another. The opposite trends in ΦPSI and ΦPSII further serves to highlight the differences between the photosystems in terms of composition and absorption. At the higher blue fractions, it is likely that cyclic electron flow was enhanced to account for the relatively increased excitation of PSII compared with PSI which may account for the slight corresponding reduction in ΦCO$_2$.

4.2. Plant growth

Since $\Phi_{CO2(LL)}$ was unaffected and integrated leaf light absorptance increased slightly with blue light fraction (Figs. 4, 5A), a likely contributor to the reduction of plant dry weight is the decrease in total plant light absorption (Fig. 6B). Similar results were reported by Hernández and Kubota (2014) for cucumber plants grown under equal light intensities with different fractions blue light. Although no differences were found in net leaf photosynthesis, biomass accumulation decreased significantly with the increase of fraction blue light due to the decrease of total plant leaf area. The linear correlation between total plant light absorption and plant dry mass production confirms the findings of Snowden et al. (2016) i.e. the effect of blue light on tomato dry mass is primarily determined by total plant light absorption rather than by direct effects on photosynthesis. Lastly, the 'sun-type' plant leaf morphology and overall phenotype resulting from high fractions of blue in some studies (e.g. Hogewoning et al., 2012) may not be advantageous for growth acclimation when plants are growing under low light intensities characteristic of the present study.

4.3. Plant development

Blue light fraction did not affect the leaf initiation rate as indicated by the unaltered leaf number (Table 1). Increasing the blue light fraction did not increase the phototropic response (and therefore the angle) of the third leaf as expected (Table 1) (Huché-Thélier et al., 2016). However, when multiple regression (ANCOVA) was used to assess the angle response of the most developed leaves (1–3 counting from the bottom), the effect of blue light fraction upon them was significant (P < 0.05).

4.4. Signalling

The linear reduction in plant height (Figs. 2A,3) due to increased blue light fraction is possibly cryptochrome-regulated (Fraser et al., 2016). This response is consistent with previous studies on tomato (Glowacka, 2004; Hernandez et al., 2016; Nanya et al., 2012; Snowden et al., 2016; Wollaeger and Runkle, 2014). The response cannot be related to phytochrome-regulated shade avoidance, since P_{fr}/P_{total} decreased by only 0.03 in the highest blue fraction treatment. Moreover, it is known that cryptochromes are the main photoreceptors inhibiting hypocotyl and epicotyl elongation, when absorbing light in the range of 390–480 nm (Ahmad and Cashmore, 1996; Ahmad et al., 2002; Hartmann, 1967). In the present study, the peak wavelength of the blue LED used was 450 nm.

5. Conclusions

The present study revealed strong photomorphogenic responses to blue light doses whereas leaf level photosynthetic responses were negligible or absent. This proved a potentially useful tool which allowed for the significance of whole plant light absorption to plant biomass to be gauged. Total dry weight of tomato plants grown under different combinations of artificial solar light enriched with blue light, while keeping photosynthetic photon flux density constant, decreased linearly as blue light fraction increased. This decrease is most likely a consequence of reduced whole plant light absorption. The fraction of blue light contained in the artificial solar light appeared to saturate all previously reported positive effects of blue light on maximum photosynthetic capacity and had no significant impact on ΦCO$_2$. When plants are

grown under constant light intensities increasing the blue light fraction in a solar light background decreases growth. This reduction in performance is primarily a consequence of the effect of blue light on plant morphology and light interception. This highlights the significance of whole plant light absorption as a major determinant of whole plant biomass but also indicates that leaf level photosynthetic effects may not reliably be extrapolated to whole plant performance in the absence of an understanding of specific effects on plant morphology and whole plant light absorption. Clearly, neither of these two factors can be viewed in isolation in relation to whole plant biomass especially since spectra which are used efficiently at the leaf level may not result in a morphology which is efficient for light capture.

Funding

CRediT authorship contribution statement

Pavlos Kalaitzoglou: Conceptualization, Methodology, Formal analysis, Writing - original draft, Visualization. **Craig Taylor:** Conceptualization, Methodology, Formal analysis, Writing - original draft, Visualization. **Kim Calders:** Methodology, Software, Resources, Data curation, Writing - original draft, Visualization. **Maikel Hogervorst:** Formal analysis, Writing - review & editing. **Wim van Ieperen:** Conceptualization, Methodology, Validation, Writing - review & editing, Supervision. **Jeremy Harbinson:** Conceptualization, Methodology, Validation, Writing - review & editing, Supervision. **Pieter de Visser:** Methodology, Software, Writing - original draft, Visualization. **Celine C. S. Nicole:** Methodology, Writing - review & editing, Supervision. **Leo F. M. Marcelis:** Conceptualization, Methodology, Validation, Writing - review & editing, Supervision, Project administration, Funding acquisition.

Declaration of Competing Interest

The authors report no declarations of interest.

Acknowledgments

Appendix A. Supplementary data

Supplementary material related to this article can be found, in the online version, at doi:https://doi.org/10.1016/j.envexpbot.2021.104377.

References

Ahmad, M., Cashmore, A.R., 1996. Seeing blue: the discovery of cryptochrome. Plant Mol. Biol. 30, 851–861.

Ahmad, M., Grancher, N., Heil, M., Black, R.C., Giovani, B., Galland, P., Lardemer, D., 2002. Action spectrum for cryptochrome-dependent hypocotyl growth inhibition in Arabidopsis. Plant Physiol. 129, 774–785.

Baker, N.R., Harbinson, J., Kramer, D.M., 2007. Determining the limitations and regulation of photosynthetic energy transduction in leaves. Plant Cell Environ. 30, 1107–1125.

Bernardini, F., Mittleman, J., Rushmeier, H., Silva, C., Taubin, G., 1999. The ball-pivoting algorithm for surface reconstruction. IEEE Trans. Vis. Comput. Graph. 5, 349–359.

Calders, K., Armston, J., Newnham, G., Herold, M., Goodwin, N., 2014. Implications of sensor configuration and topography on vertical plant profiles derived from terrestrial LiDAR. Agric. For. Meteorol. 194, 104–117.

Calders, K., Newnham, G., Burt, A., Murphy, S., Raumonen, P., Herold, M., Culvenor, D., Avitabile, V., Disney, M., Armston, J., Kaasalainen, M., 2015. Nondestructive estimates of above-ground biomass using terrestrial laser scanning. Methods Ecol. Evol. 6, 198–208.

Calders, K., Disney, M.I., Armston, J., Burt, A., Brede, B., Origo, N., Muir, J., Nightingale, J., 2017. Evaluation of the range accuracy and the radiometric calibration of multiple terrestrial laser scanning instruments for data interoperability. IEEE Trans. Geosci. Remote. Sens. 55, 2716–2724.

Chow, W.S., Melis, A., Anderson, J.M., 1990. Adjustments of photosystem stoichiometry in chloroplasts improve the quantum efficiency of photosynthesis. Proc. Natl. Acad. Sci. U. S. A. 87, 7502–7506.

Croce, R., Müller, M.G., Bassi, R., Holzwarth, A.R., 2001. Carotenoid-to-chlorophyll energy transfer in recombinant major light-harvesting complex (LHCII) of higher plants. I. Femtosecond transient absorption measurements. Biophys. J. 80, 901–915.

Farquhar, G.D., von Caemmerer, S., Berry, J.A., 1980. A biochemical model of photosynthetic CO2 assimilation in leaves of C 3 species. Planta 149, 78–90.

Fraser, D.P., Hayes, S., Franklin, K.A., 2016. Photoreceptor crosstalk in shade avoidance. Curr. Opin. Plant Biol. 33, 1–7.

Glowacka, B., 2004. The effect of blue light on the height and habit of the tomato (*Lycopersicon esculentum* Mill.) transplant. Folia Hortic. 16, 3–10.

Hartmann, K.M., 1967. [An action spectrum of photomorphogenesis under high energy conditions and its interpretation on the basis of phytochrome (hypocotyl growth inhibition in Lactuca sativa L)]. Z. Naturforsch. B 22, 1172–1175.

Hernández, R., Kubota, C., 2014. Growth and morphological response of cucumber seedlings to supplemental red and blue photon flux ratios under varied solar daily light integrals. Sci. Hortic.-Amsterdam 173, 92–99.

Hernández, R., Kubota, C., 2016. Physiological responses of cucumber seedlings under different blue and red photon flux ratios using LEDs. Environ. Exp. Bot. 121, 66–74.

Hernandez, R., Eguchi, T., Deveci, M., Kubota, C., 2016. Tomato seedling physiological responses under different percentages of blue and red photon flux ratios using LEDs and cool white fluorescent lamps. Sci. Hortic.-Amsterdam 213, 270–280.

Hogewoning, S.W., Douwstra, P., Trouwborst, G., van Ieperen, W., Harbinson, J., 2010a. An artificial solar spectrum substantially alters plant development compared with usual climate room irradiance spectra. J. Exp. Bot. 61, 1267–1276.

Hogewoning, S.W., Trouwborst, G., Maljaars, H., Poorter, H., van Ieperen, W., Harbinson, J., 2010b. Blue light dose-responses of leaf photosynthesis, morphology, and chemical composition of Cucumis sativus grown under different combinations of red and blue light. J. Exp. Bot. 61, 3107–3117.

Hogewoning, S.W., Wientjes, E., Douwstra, P., Trouwborst, G., van Ieperen, W., Croce, R., Harbinson, J., 2012. Photosynthetic quantum yield dynamics: from photosystems to leaves. Plant Cell 24, 1921–1935.

Hoover, W.H., 1937. The Dependence of Carbon Dioxide Assimilation in a Higher Plant on Wave Length of Radiation. Smithsonian Institution, Washington.

Huché-Thélier, L., Crespel, L., Gourrierec, J.L., Morel, P., Sakr, S., Leduc, N., 2016. Light signaling and plant responses to blue and UV radiations—perspectives for applications in horticulture. Environ. Exp. Bot. 121, 22–38.

Inada, K., 1976. Action spectra for photosynthesis in higher-plants. Plant Cell Physiol. 17, 355–365.

Kaiser, E., Ouzounis, T., Giday, H., Schipper, R., Heuvelink, E., Marcelis, L.F.M., 2019. Adding blue to red supplemental light increases biomass and yield of greenhouse-grown tomatoes, but only to an optimum. Front. Plant Sci. 9, 2002.

Keller, M.M., Jaillais, Y., Pedmale, U.V., Moreno, J.E., Chory, J., Ballare, C.L., 2011. Cryptochrome 1 and phytochrome B control shade-avoidance responses in Arabidopsis via partially independent hormonal cascades. Plant J. 67, 195–207.

Keuskamp, D.H., Sasidharan, R., Vos, I., Peeters, A.J., Voesenek, L.A., Pierik, R., 2011. Blue-light-mediated shade avoidance requires combined auxin and brassinosteroid action in Arabidopsis seedlings. Plant J. 67, 208–217.

Keuskamp, D.H., Keller, M.M., Ballare, C.L., Pierik, R., 2012. Blue light regulated shade avoidance. Plant Signal. Behav. 7, 514–517.

Kingston-Smith, A.H., Harbinson, J., Foyer, C.H., 1999. Acclimation of photosynthesis, H2O2 content and antioxidants in maize (Zea mays) grown at sub-optimal temperatures. Plant Cell Environ. 22, 1071–1083.

Kniemeyer, O., 2008. Design and Implementation of a Graph Grammar Based Language for Functional-structural Plant Modelling., Fakultät Für Mathematik, Naturwissenschaften Und Informatik. Brandenburg University of Technology, Cottbus.

Kok, B., 1948. A Critical Consideration of the Quantum Yield of Chlorella Photosynthesis. Enzymologia. Junk, W., p. 56

Laisk, A., Oja, V., Eichelmann, H., Dall'Osto, L., 2014. Action spectra of photosystems II and I and quantum yield of photosynthesis in leaves in State 1. Biochim. Biophys. Acta 1837, 315–325.

Lichtenthaler, H.K., Buschmann, C., Rahmsdorf, U., 1980. The importance of Blue light for the development of sun-type chloroplasts. In: Senger, H. (Ed.), The Blue Light Syndrome. Springer Berlin Heidelberg, Berlin, Heidelberg, pp. 485–494.

Matsuda, R., Ohashi-Kaneko, K., Fujiwara, K., Goto, E., Kurata, K., 2004. Photosynthetic characteristics of rice leaves grown under red light with or without supplemental blue light. Plant Cell Physiol. 45, 1870–1874.

Matsuda, R., Ohashi-Kaneko, K., Fujiwara, K., Kurata, K., 2007. Analysis of the relationship between blue-light photon flux density and the photosynthetic properties of spinach (Spinacia oleracea L.) leaves with regard to the acclimation of photosynthesis to growth irradiance. Soil Sci. Plant Nutr. 53, 459–465.

McCree, K.J., 1971. The action spectrum, absorptance and quantum yield of photosynthesis in crop plants. Agric. Meteorol. 9, 191–216.

Meshlab, 2014. Visual Computing Lab - ISTI - CNR.

Nagashima, H., Hikosaka, K., 2011. Plants in a crowded stand regulate their height growth so as to maintain similar heights to neighbours even when they have potential advantages in height growth. Ann. Bot. 108, 207–214.

Nanya, K., Ishigami, Y., Hikosaka, S., Goto, E., 2012. Effects of Blue and Red Light on Stem Elongation and Flowering of Tomato Seedlings, 956 ed. International Society for Horticultural Science (ISHS), Leuven, Belgium, pp. 261–266.

Pierik, R., Djakovic-Petrovic, T., Keuskamp, D.H., de Wit, M., Voesenek, L.A.C.J., 2009. Auxin and ethylene regulate elongation responses to neighbor proximity signals independent of gibberellin and DELLA proteins in Arabidopsis. Plant Physiol. 149, 1701–1712.

Poorter, H., Niinemets, U., Poorter, L., Wright, I.J., Villar, R., 2009. Causes and consequences of variation in leaf mass per area (LMA): a meta-analysis. New Phytol. 182, 565–588.

R Development Core Team, 2010. R: a Language and Environment for Statistical Computing. R Foundation of Statistical Computing, Vienna, Austria.

Sager, J.C., Smith, W.O., Edwards, J.L., Cyr, K.L., 1988. Photosynthetic efficiency and phytochrome photoequilibria determination using spectral data. Trans. ASAE 31, 1882–1889.

Sarlikioti, V., de Visser, P.H.B., Buck-Sorlin, G.H., Marcelis, L.F.M., 2011. How plant architecture affects light absorption and photosynthesis in tomato: towards an ideotype for plant architecture using a functional-structural plant model. Ann Bot-London 108, 1065–1073.

Sharkey, T.D., Raschke, K., 1981. Effect of light quality on stomatal opening in leaves of Xanthium strumarium l. Plant Physiol. 68, 1170–1174.

Smith, H., 1982. Light quality, photoperception, and plant strategy. Annu. Rev. Plant Phys. 33, 481–518.

Snowden, M.C., Cope, K.R., Bugbee, B., 2016. Sensitivity of seven diverse species to blue and green light: interactions with photon flux. PLoS One 11, 32.

Sonneveld, P.J., Swinkels, G.L.A.M., Kempkes, F., Campen, J.B., Bot, G.P.A., 2006. Greenhouse With an Integraged NIR Filter and a Solar Cooling System, 719 ed. International Society for Horticultural Science (ISHS), Leuven, Belgium, pp. 123–130.

Suetsugu, N., Wada, M., 2013. Evolution of three LOV blue light receptor families in green plants and photosynthetic stramenopiles: phototropin, ZTL/FKF1/LKP2 and aureochrome. Plant Cell Physiol. 54, 8–23.

Taylor, C.R., van Ieperen, W., Harbinson, J., 2019. Demonstration of a relationship between state transitions and photosynthetic efficiency in a higher plant. Biochem. J. 476, 3295–3312.

Thornley, J.H.M., 1976. Mathematical Models in Plant Physiology: a Quantitative Approach to Problems in Plant and Crop Physiology / J. H. M. Thornley. Thornley. Academic Press, London, New York.

Wickham, H., 2016. ggplot2: Elegand Graphics for Data Analysis. Springer-Verlag, New York.

Wollaeger, H.M., Runkle, E.S., 2014. Growth of impatiens, Petunia, Salvia, and tomato seedlings under blue, Green, and red light-emitting diodes. HortScience 49, 734–740.